Title:

Fork restart protein, PriA, binds around *oriC* after depletion of nucleotide precursors: replication fork arrest near the replication origin

Taku Tanaka[1], Yasumasa Nishito[2], and Hisao Masai[1]

From [1]Department of Genome Medicine and [2]Basic Technology Research Center, Tokyo Metropolitan Institute of Medical Science, 4-6-1 Kamiktazawa, Setagaya-ku, Tokyo 156-8506, JAPAN

Running title: Replication fork arrest near *oriC*

Correspondence should be addressed to
Hisao Masai
E-mail: masai-hs@igakuken.or.jp
Telephone: +81-3-5316-3231
Fax: +81-3-5316-3145

Abstract

Arrest of replication fork progression is one of the most common causes for increasing the genomic instability. In bacteria, PriA, a conserved DEXH-type helicase, plays a major role in recognition of the stalled forks and restart of DNA replication. We took advantage of PriA's ability to specifically recognize stalled replication forks to determine the genomic loci where replication forks are prone to stall on the *Escherichia coli* genome. We found that PriA binds around *oriC* upon thymine starvation which reduces the nucleotide supply and causes replication fork stalling. PriA binding quickly disappeared upon readdition of thymine. Furthermore, BrdU was incorporated at around *oriC* upon release from thymine starvation. Our results indicate that reduced supply of DNA replication precursors causes replication fork stalling preferentially in the 600 kb segment centered at *oriC*. This suggests that replication of the vicinity of *oriC* requires higher level of nucleotide precursors. The results also point to a possibility of slow fork movement and/ or the presence of multiple fork arrest signals within this segment. Indeed, we have identified rather strong fork stall/ pausing signals symmetrically located at ~50 kb away from *oriC*. We speculate that replication pausing and fork-slow-down shortly after initiation may represent a novel checkpoint that ensures the presence of sufficient nucleotide supply prior to commitment to duplication of the entire genome.

Key words: genome stability/stalled replication fork/*oriC*/PriA/eCOMB

Highlights

1 Upon thymine starvation, PriA protein binds around *oriC*, suggesting that replication forks stall preferentially near *oriC* shortly after initiation.
2 PriA dissociates from *oriC* upon readdition of thymine to thymine-starved cells.
3 BrdU incorporation assays show forks are restarted at around *oriC* after release from thymine starvation, consistent with the fork stall near *oriC*.
4 Symmetrically located specific replication fork pause/ arrest sites were detected at ~50 kb away from *oriC* in unperturbed growth.

Introduction

Various internal and external insults can stall the progression of replication forks, which could threaten the stable maintenance of genomes [1-3]. Indeed, it has been reported that oncogenic stress induces DNA replication stress in very early stages of tumorigenesis, and loss of proper cellular responses to replication fork stalling leads to more extensive genomic instability and tumor progression [4,5]. Normal cells are equipped with layers of protective systems that deal with the replication failure to overcome the fork blocks and facilitate the completion of the replication of the entire genome.

In bacteria, where replication is normally initiated at a single loci, stalled forks cannot be rescued by another replication fork, unlike in the case for eukaryotic cells. Thus, replication fork restart plays a major role in dealing with a stalled replication fork [6,7]. PriA, originally discovered as a factor essential for conversion of single-stranded ϕX174 phage to duplex RF form, has been known to play essential roles fork restart reaction in *E. coli* [7,8]. PriA recognizes stalled forks by specifically recognizing the 3'-hydroxyl group at the nascent leading strand at the branch point [7, 9-11]. Although PriC-dependent system can restart the fork *in vitro* from a stalled fork with a single-stranded gap on the leading strand template [12,13], *priC* null mutant is not defective in fork restart [14]. Thus, the PriA pathway plays a major role in fork restart in cells. Fork regression through multiple pathways would bring the 3'-hydroxyl group of the leading strand to the branchpoint, generating an optimum substrate for PriA-dependent fork restart [7].

On the eukaryotic genomes, regions where genomes are more vulnerable to genotoxic stress have been identified. These regions are often late-replicating and are prone to stall the replication fork more frequently than others. They may also be slow-replicating segments (replication slow zones [RSZs] in budding yeast; 15). On mammalian genomes, they are known as fragile sites [16]. Extreme high-affinity of PriA to the stalled DNA fork structure prompted us to search for similar segments on the *E. coli* genome by determining genome-wide PriA binding sites through ChIP analyses using PriA antibody.

PriA did not bind to specific genomic segments during normal growth, but bound around *oriC* upon thymine starvation that limits the amount of DNA replication

precursors. Direct labeling of nascent DNA with BrdU after release from thymine starvation and immunoprecipitation of the labeled DNA also indicates stalling of replication forks near *oriC*. Analyses of DNA synthesis with unperturbed *E. coli* cells suggest the presence of fork arrest signals and slow replication fork progression in this segment even during the normal growth. The results suggest potential novel regulation of replication fork progression in the vicinity of *oriC*.

Materials and Methods is described in Supplementary Materials.

Results

Development of antibody against *E. coli* PriA protein

In order to conduct ChIP analyses of PriA protein, we have developed specific antibody. We overexpressed the full-length PriA protein, purified it and used as an antigen to develop rabbit polyclonal antibody against PriA. The serum was further affinity-purified by the antigen protein. The serum and purified antibody were used to detect PriA protein in the total lysate of *E. coli* cells as well as in the immunoprecipitated fractions. PriA in the lysate was detected by both antibody solutions. Non-specifically reacting band at ~120 kDa detected by serum did not appear with the purified antibody. Lower molecular weight bands detected in the immunoprecipitates probably represent the heavy chains and their degradations. PriA was not detected in the supernatant of the immunoprecipitation when the purified antibody was used, suggesting that the efficiency of immunoprecipitation is quite high (**Supplementary Figure S1**). The antibody was used also for immunostaining. The endogenous PriA signal was detected along the entire nucleoid. The signal was lost or significantly reduced in *priA* null cells (**Supplementary Figure S2**), validating the signals.

Next, using the affinity-purified antibody, we examined whether thymine starvation affects the abundance of PriA protein. We did not see any effect of thymine starvation on the level of the endogenous PriA protein, consistent with the absence of SOS-responsive elements in the promoter region for *priA* (**Figure 1 A-D**).

ChIP-chip analyses of PriA binding after thymine starvation and release.

We conducted the ChIP-chip analyses using the developed PriA antibody to determine the PriA binding locations before and after thymine starvation. We used *thyA* cells, which requires thymine in the media for growth due to mutation in thymidylate synthase. In this strain, depletion of thymine in the medium results in limited supply of TTP, leading to replication fork arrest. There was no significant chromatin binding of PriA in unperturbed growth, as expected from its role in replication fork stress condition. In contrast, PriA bound to the *oriC* region after thymine starvation. Binding summit was at around *oriC* and binding was distributed for 200-300 kb (or sometimes more) on both sides (**Figures 1E, 2A**). This peak was not detected in PriA null cells, verifying the authenticity of the signals (**Figure 1F**).

When cells were released from thymine starvation, the observed PriA binding gradually decreased and was almost gone in 10 min after release (**Figure 2A**). The binding of PriA to the *oriC* region after thymine starvation and its dissociation after the release was verified by qPCR analyses of ChIP signals (**Figure 2B**). The result suggests that DNA replication is restarted from the arrested replication forks, which may represent iSDR (inducible Stable DNA Replication) [17], but is not initiated at oriC, since release was conducted in the presence of rifampicin and chloramphenicol, the inhibitors of transcription and protein synthesis, respectively. This result also indicates that PriA is no longer needed after replication restart, consistent with its role as a recruiter of the DnaB helicase [18].

We did not see any significant PriA binding to *ter* sequences, although it is known that *ter* can block DNA replication in the cells [19]. This may be because fork arrest at *ter* may be very rare events during normal growth. Alternatively, the *ter*-tus system normally mediates “programmed” fork arrest which may not elicit PriA binding probably because the forks are “protected”.

Genome-wide thymidine incorporation in release from thymine starvation and in unperturbed growth

We then used eCOMB [20], in which genetic modification permits efficient incorporation of thymidine derivatives including BrdU, to directly measure DNA synthesis. BrdU was incorporated around *oriC*, in the first 2 min after release from thymine starvation in the presence of chloramphenicol (**Figure 3, upper [red]**), consistent with resumption of DNA synthesis from the arrested forks accumulated

around *oriC*. When exponentially growing cells were labeled with BrdU, we observed a valley of incorporation in the region centered at *oriC* (~600 kb wide). This result indicates that the relative ratio of newly synthesized DNA to the total amount of genomic DNA is low over the ~600 kb segments surrounding *oriC* (**Figure 3, lower [green]**). The genome-wide analyses of copy number have shown general increase of the copy number around *oriC*, reflecting the initiation of DNA replication [21-23]. The values shown in our ChIP results are the ChIP signals corrected by the input genomic DNA, and thus the copy number increase could account for lower signals in the *oriC* region. However, the signal reduction was more than two-fold, pointing to decreased rate of BrdU incorporation around *oriC* compared to other segments. Interestingly, a small peak was observed at *oriC* along with the two sharp bottom points symmetrically located relative to *oriC* (~50 kb away from *oriC*; **Figure 3, lower [green]**). This suggests the presence of fork blocks on both sides of *oriC* and the neighboring slow-replicating segments of 600 kb. Interestingly, the fork blocks appear to function only in the unperturbed growth. We did not observe any "valley" of BrdU incorporation in release from thymine starvation (**Figure 3A**). We also observed a small peak of BrdU incorporation near *ter* after thymine starvation. This may represent replication from "*oriK*", putative replication origins for iSDR [22]

Discussion

PriA is conserved throughout the eubacteria and plays essential roles in restart of stalled replication forks [7,8]. *In vitro* it binds to arrested fork DNA containing 3'-hydroxyl group of the nascent leading strand at the branch point with a high affinity. Here we attempted to determine the fork-stall sites on the *E. coli* genome by analyzing the *in vivo* binding sites of PriA by ChIP. We first developed a specific antibody and validated it. The developed antibody is highly specific to PriA protein and works for Western, immunoprecipitation, and immunostaining (**Figures 1, S1 and S2**).

We induced replication fork arrest by starving thymine from the media in *thyA* cells. This treatment is known to induce iSDR [17]. Unexpectedly, we have observed significant PriA binding around *oriC* after thymine starvation (**Figures 1 and 2**). Since we did not synchronize the cell cycle, this means that replication forks tend to stall shortly after initiation at *oriC* under the condition where the supply of materials for

DNA synthesis are limited, while they can proceed through other segments of the genome. The width of the PriA binding peak is ~600 kb. Similarly, BrdU incorporation after thymine starvation peaked at *oriC* and extended over a 600 kb segment (**Figure 3**). Similar PriA binding around *oriC* was observed also in cells treated with hydroxyurea (an inhibitor of ribonucleotide reductase known to inhibit DNA replication by depletion of dNTPs; **Figure 4**). This suggests that higher concentration of nucleotide precursors may be required for the replication of the *oriC*-proximal segments. In contrast to thymine starvation or HU treatment, UV irradiation did not result in binding of PriA at any specific locations on the genome (**Figure 4**), suggesting that forks may be more stochastically stalled on the entire genome after UV treatment.

Upon addition of thymine, replication restarted and PriA binding around *oriC* was lost. The binding mostly disappeared in 10 min. Assuming the 200 kb segment is replicated during 10 min, the average fork rate is 20 kb/min (330 bp/sec), which is about a half of the known fork movement rate in *E. coli* [20], suggesting that the fork moves slowly in the vicinity of *oriC*.

We have identified the two bottoms of BrdU incorporation after 2 min labeling of the exponentially growing eCOMB cells that are located symmetrically at ~50 kb away from *oriC*. This may represent a Tus-*ter*-like programmed replication termination (pausing) event, although we did not find *ter*-related sequences in the corresponding regions. The low rate of BrdU incorporation around *oriC* is consistent with the slow fork movement near *oriC*.

It has been known that thymine starvation induces thymineless death in *E. coli thyA* mutant cells [21]. It was recently reported that the specific loss of the genome segments surrounding *oriC* correlates with the cell death induced by thymine starvation [21, 24]. Under our experimental conditions, no significant loss of cell viability is observed after thymine starvation (data not shown). PriA binding to *oriC* is observed also after HU treatment (**Figure 4**). Thus, PriA binds to stalled replication forks around *oriC*, but not to the fragmented *oriC* DNA that may have been caused by thymine starvation. The unusual pattern of BrdU incorporation around *oriC* in unperturbed *E. coli* cells also indicates the presence of intrinsic unique replication fork regulation near *oriC*. However, it would be possible that degradation of the *oriC*-proximal sequences after prolonged thymine starvation may be triggered by fork-stalling nature of these sequences.

The mechanism for fork stall around *oriC* under limited nucleotide supply is not clear at the moment. However, it would be worthwhile to point out a few possibilities. *E. coli* chromosomes are known to be composed of macrodomains, which may constitute chromosome structural and functional units [25-27]. The sequences near *oriC* generate a specific macrodomain structures that may generate a spatially secluded domain. This special domain may be related to intrinsic slow fork movement around *oriC*. It is also known that the two replisomes colocalize immediately after the initiation at *oriC* [28,29]. The clustering of the replisomes may result in rapid depletion of nucleotide pools locally around *oriC*, causing preferential fork arrest under nucleotide depletion. More detailed characterization of chromatin structures around *oriC* would be needed to test these possibilities.

In summary, we show here that PriA binds around *oriC* after replication fork block caused by reduced nucleotide precursors. It appears that higher concentration of nucleotide precursors are required to go through the replication of initial ~600 kb after initiation at *oriC*. There may be strong fork arrest signals ~50 kb away from o*riC* that may function primarily during unperturbed growth. In addition, the initial ~600 kb may be replicated more slowly than other segments. Alternatively, there may be multiple weak fork barriers in the ~600 kb segment centered at *oriC*, which may pause or slow down the moving replication forks. The significance and mechanism of this replication fork regulation are not clear at the moment. It may represent the additional layer of a checkpoint regulation that may ensure the presence of sufficient level of nucleotide precursors before commitment to entry into the "no-return" replication cycle of the entire genome. In eukaryotes, addition of hydroxyurea to asynchronous cultures results in uniform arrest in early S phase with limited replication from early-firing origins. This situation is very similar to what we have observed in *E. coli,* suggesting that similar regulation may operate in eukaryotes as well. Dr. Masahiro Akiyama and his colleagues also made similar findings in their independent studies (Akiyama *et al*., personal communication).

Supplementary Materials for this article is available online.

Acknowledgements

We would like to thank Drs. Masahiro Akiyama and Hisaji Maki for the generous gift of eCOMB strain and for communication of unpublished data. We also greatly thank Drs. Tsutomu Katayama and Hironori Kawakami for various strains and helpful discussion. We would like especially thank Dr. Tsutomu Katayama for very useful suggestions on the manuscript. We would also like to thank Drs. Nobuaki Kohno and Taku Oshima for their advice on processing of the genome-wide data. We would like to thank all the members of the laboratory for help and discussion. This work was supported by JSPS KAKENHI (Grant-in-Aid for Scientific Research (A) [Grant Numbers 23247031 and 26251004] and Grant-in-Aid for Scientific Research on Priority Areas ["non-coding RNA" and "Genome Adaptation"; Grant Numbers 24114520 and 25125724, respectively] to H.M.

References

1. Branzei D, Foiani M (2010) Maintaining genome stability at the replication fork. Nat Rev Mol Cell Biol 11: 208-219

2. Cox MM, Goodman MF, Kreuzer KN, Sherratt DJ, Sandler SJ, Marians KJ (2000) The importance of repairing stalled replication forks. Nature 404: 37-41

3. Zeman MK, Cimprich KA (2014) Causes and consequences of replication stress. Nat Cell Biol 16: 2-9

4. Gorgoulis VG, Vassiliou LV, Karakaidos P, Zacharatos P, Kotsinas A, Liloglou T, Venere M, Ditullio RA Jr, Kastrinakis NG, Levy B, Kletsas D, Yoneta A, Herlyn M, Kittas C, Halazonetis TD (2005) Activation of the DNA damage checkpoint and genomic instability in human precancerous lesions. Nature 434: 907-913

5. Bartkova J, Horejsí Z, Koed K, Krämer A, Tort F, Zieger K, Guldberg P, Sehested M, Nesland JM, Lukas C, Ørntoft T, Lukas J, Bartek J (2005) DNA damage response as a candidate anti-cancer barrier in early human tumorigenesis. Nature 434: 864-870

6. Heller RC, Marians KJ (2006) Replisome assembly and the direct restart of stalled replication forks. Nat Rev Mol Cell Biol 12: 932-943

7. Masai H, Tanaka T, Kohda D (2010) Stalled replication forks: making ends meet for recognition and stabilization. Bioessays 32: 687-697

8. Marians KJ (2000) PriA-directed replication fork restart in Escherichia coli. Trends Biochem Sci 25: 185-189

9. Mizukoshi T, Tanaka T, Arai K, Kohda D, Masai H (2003) A critical role of the 3' terminus of nascent DNA chains in recognition of stalled replication forks. J Biol Chem 278: 42234-42239

10. Tanaka T, Masai H (2006) Stabilization of a stalled replication fork by concerted actions of two helicases. J Biol Chem 281: 3484-3493

11. Sasaki K, Ose T, Okamoto N, Maenaka K, Tanaka T, Masai H, Saito M, Shirai T, Kohda D (2007) Structural basis of the 3'-end recognition of a leading strand in stalled replication forks by PriA. EMBO J 26: 2584-2593

12. Heller RC, Marians KJ (2005) The disposition of nascent strands at stalled replication forks dictates the pathway of replisome loading during restart. Mol Cell 17: 733-743.

13. Sandler SJ (2000) Multiple genetic pathways for restarting DNA replication forks in *Escherichia coli* K-12. Genetics 155: 487-497

14. Sandler SJ, Marians KJ, Zavitz KH, Coutu J, Parent MA, Clark AJ. (1999) dnaC mutations suppress defects in DNA replication- and recombination-associated functions in priB and priC double mutants in Escherichia coli K-12. Mol Microbiol 34:91-101

15. Cha RS, Kleckner N (2002) ATR homolog Mec1 promotes fork progression, thus averting breaks in replication slow zones. Science 297:602-606

16. Debatisse M, Le Tallec B, Letessier A, Dutrillaux B, Brison O (2012) Common fragile sites: mechanisms of instability revisited. Trends Genet 28:22-32

17. Kogoma T (1997) Stable DNA replication: interplay between DNA replication, homologous recombination, and transcription. Microbiol Mol Biol Rev 61: 212-238

18. Manhart CM, McHenry CS (2015) Identification of subunit binding positions on a model fork and dsplacements that occur during sequential assembly of the *Escherichia coli* primosome. J Biol Chem 290: 10828-10839

19. Rudolph CJ, Upton AL, Stockum A, Nieduszynski CA, Lloyd RG (2013) Avoiding chromosome pathology when replication forks collide. Nature 500: 608-611

20. Pham TM, Tan KW, Sakumura Y, Okumura K, Maki H, Akiyama MT (2013) A single-molecule approach to DNA replication in *Escherichia coli* cells demonstrated that DNA polymerase III is a major determinant of fork speed. Mol Microbiol 90: 584-596.

21. Kuong KJ, Kuzminov A (2012) Disintegration of nascent replication bubbles during thymine starvation triggers RecA- and RecBCD-dependent replication origin destruction. J Biol Chem 287: 23958-23970

22. Maduike NZ, Tehranchi AK, Wang JD, Kreuzer KN (2014) Replication of the Escherichia coli chromosome in RNase HI-deficient cells: multiple initiation regions and fork dynamics. Mol Microbiol 91: 39-56

23. Dimude JU, Stockum A, Midgley-Smith SL, Upton AL, Foster HA, Khan A, Saunders NJ, Retkute R, Rudolph CJ (2015) The consequences of replicating in the wrong orientation: bacterial chromosome duplication without an active replication origin. MBio 6: e01294-01315

24. Sangurdekar DP, Hamann BL, Smirnov D, Srienc F, Hanawalt PC, Khodursky AB (2010) Thymineless death is associated with loss of essential genetic information from the replication origin. Mol Microbiol 75:1455-1467

25. Valens M, Penaud S, Rossignol M, Cornet F, Boccard F. (2004) Macrodomain organization of the Escherichia coli chromosome. EMBO J. 23: 4330-4341

26. Dame RT, Kalmykowa OJ, Grainger DC. (2011) Chromosomal macrodomains and associated proteins: implications for DNA organization and replication in gram negative bacteria. PLoS Genet. 7: e1002123.

27. Esnault E, Valens M, Espéli O, Boccard F. (2007) Chromosome structuring limits genome plasticity in Escherichia coli. PLoS Genet. 3: e226.

28. Sunako Y, Onogi T, Hiraga S. (2001) Sister chromosome cohesion of Escherichia coli. Mol Microbiol. 42: 1233-12341.

29. Ozaki S, Matsuda Y, Keyamura K, Kawakami H, Noguchi Y, Kasho K, Nagata K, Masuda T, Sakiyama Y, Katayama T. (2013) A replicase clamp-binding dynamin-like protein promotes colocalization of nascent DNA strands and equipartitioning of chromosomes in E. coli. Cell Rep. 4: 985-995.

30. Tanaka T, Mizukoshi T, Taniyama C, Kohda D, Arai K, Masai H (2002) DNA binding of PriA protein requires cooperation of the N-terminal D-loop/arrested-fork binding and C-terminal helicase domains. J Biol Chem 277: 38062-38071

31. Hayashi K, Morooka N, Yamamoto Y, Fujita K, Isono K, Choi S, Ohtsubo E, Baba T, Wanner BL, Mori H, Horiuchi T. (2006) Highly accurate genome sequences of *Escherichia coli* K-12 strains MG1655 and W3110. Mol Syst Biol 2: 0007

32. Hill CW, Harnish BW (1981) Inversions between ribosomal RNA genes of *Escherichia coli*. Proc Natl Acad Sci U S A 78:7069-7072

33. Hiraga S, Ichinose C, Niki H, Yamazoe M (1998) Cell cycle–dependent duplication and bidirectional migration of SeqA-associated DNA–protein complexes in *E. coli.* Mol Cell 1: 381–387

34. Lee EH, Masai H, Allen GC Jr, Kornberg A (1990) The *priA* gene encoding the primosomal replicative n' protein of *Escherichia coli*. Proc Natl Acad Sci U S A 87: 4620-4624

35. Masai H, Asai T, Kubota Y, Arai K, Kogoma T (1994) *Escherichia coli* PriA protein is essential for inducible and constitutive stable DNA replication. EMBO J 13: 5338–5345

36. Nishida S, Fujimitsu K, Sekimizu K, Ohmura T, Ueda T, Katayama T (2002) A nucleotide switch in the *Escherichia coli* DnaA protein initiates chromosomal replication. J Biol Chem 277: 14986-14995

Legends to Figures

Figure 1. Development of anti-PriA protein antibody and ChIP-on-chip analysis of PriA protein chromatin binding after thymine starvation.

The newly developed anti-PriA antibody was used in immunoprecipitation (IP) experiments. Immunoprecipitated proteins were analyzed on SDS-PAGE and were detected with silver staining (A and C) or western blotting (B and D). (A) Proteins immunoprecipitated with anti-PriA antibody or control IgG from normally growing cells (in LB medium). (B) The same fractions (as in A) were analyzed by western blotting using the anti-PriA antibody. (C) The immunoprecipitated proteins from normally growing or thymine-starved cells. (D) The immunoprecipitated proteins (as in C) were analyzed by western blotting. The position of PriA is indicated by arrow. In (B) and (D), purified PriA protein (1 ng) was also loaded as a control (lane 1). Precipitated PriA protein is indicated by arrows. In (B) and (D), affinity-purified anti-PriA antibody was used for Western analyses. In (E) and (F), chromatin immunoprecipitation (ChIP) with the affinity-purified anti-PriA antibody was conducted with the indicated strains. (E) AQ634 (*priA*$^{+}$ *thyA*). Red, cells exponentially growing in M9 medium at 30°C; blue, cells washed and released into M9 without thymine for 3 hrs. Genomic DNA was extracted and fragmented before immunoprecipitation with anti-PriA antibody for microarray analyses. (F) AQ8851 (*priA1::kan thyA*) cells were treated and analyzed as described in E. Purple, exponentially growing; light blue, thymine starved. Intensity of the signal from ChIPed sample was divided by that from the input DNA and values were plotted as log ratio on the whole genome scale. Moving average was calculated and drawn as thick line (window size, 1 kb). The positions of *oriC* and *ter* sequences are indicated. Note that about 800kb sequences surrounding *oriC* (shown by a double-arrowed line) are inverted on the map in this figure and in Figures 2A, 3 and 4, because W3110 was used as a reference genome (see also "Materials and methods"). Tall spikes are noise signals.

Figure 2 ChIP-on-chip analysis of PriA protein chromatin binding after release from thymine starvation.

(A) KH5402-1 (*thyA*) cells were treated and analyzed as described in A. Brown, exponentially growing; dark blue, thymine starved; blue-green, released for 5 min;

dark-green, released for 10 min. Intensity of the signal from IP sample was divided by that from input DNA and values are plotted as log ratio on the whole genome scale. Intensity of the signal from ChIPed sample was divided by that from the input DNA and values were plotted as log ratio on the whole genome scale. Moving average was calculated and drawn as thick line (window size, 1 kb). The positions of *oriC* and ter sequences are indicated. (B) KH5402-1 was grown in M9 media without thymine for 3 h and transferred to the media containing 8 μg/ml of thymine along with with 200 μg/ml of rifampicin and 150 μg/ml of chloramphenicol to restart DNA synthesis (iSDR). Cells were collected at the indicated time (0 [red], 10 [pink] and 20 [pale red] min) and fixed for lysate preparation before ChIP analysis. Quantitative PCR was conducted with ChIPed samples from cells indicated. The position of each primer set is indicated at the bottom on the genome scale bar. Values from the anti-PriA antibody ChIPed samples were divided with those from IgG ChIPed samples.

Figure 3. BrdU incorporation in cells released from thymine starvation and in those growing exponentially. eCOMB (Δ*thyA* Δ*yjjG-deoB*) cells were grown in M9CAA with tryptophan and washed with M9 salt, and incubated without thymine for 3 hrs. Cells were then released into media containing 50 μg/ml BrdU and 150 μg/ml chloramphenicol for 2 min, and then NaN3 was added at 2%. Cells (200 ml) were harvested and DNA was sheared by sonication. Purified fragmented DNA was immunoprecipitated with 2 μg of anti-BrdU antibody and the precipitated DNA was analyzed on microarray after amplification (red; release from thymine starvation). eCOMB cells (50 ml) growing exponentially were labeled with 50 μg/ml BrdU for 5 min, and then cells were treated as above (green; normal growth). Intensity of the signal from anti-BrdU antibody ChIPed sample was divided by that from the input DNA and values were plotted as log ratio on the whole genome scale. Moving average was calculated and drawn as thick line (window size, 1 kb). The positions of *ter* sequences and *oriC* are marked on the genome scale bar.

Figure 4. ChIP-on-chip analysis of PriA protein chromatin binding in the presence of HU or after treatment with UV.

Chromatin immunoprecipitation (ChIP) with anti-PriA antibody was conducted with AQ634 (*priA*$^{+}$ *thyA*). Red, cells exponentially growing in M9 medium at 30°C; blue,

cells washed and released into M9 without thymine for 3 hrs. The same strain was treated with UV and incubated in the same medium for 70 min (purple; see "Materials and methods"), or incubated in the presence of 80 mM HU for 4 hrs (green). Genomic DNA was extracted and fragmented before immunoprecipitation with anti-PriA antibody for microarray analyses. Intensity of the signal from ChIPed sample was divided by that from the input DNA and values were plotted as log ratio on the whole genome scale. Moving average was calculated and drawn as thick line (window size, 1 kb). The positions of *oriC* and *ter* sequences are indicated.

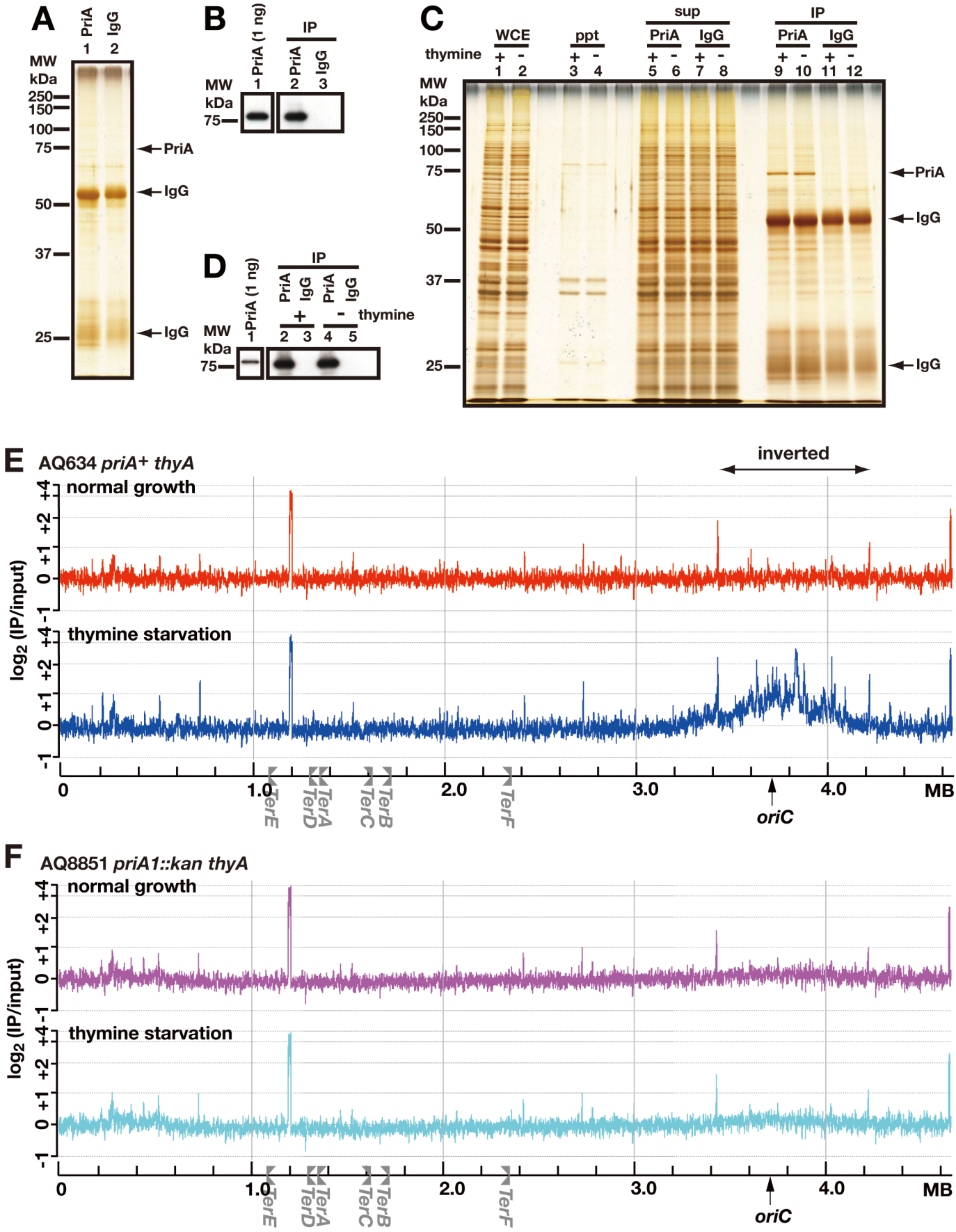
A
PriA
IgG
1
2
MW
kDa
250
150
100
75
50
37
25
PriA
IgG
IgG
B
PriA (1 ng)
IP
PriA
IgG
2
3
C
thymine
WCE
ppt
sup
PriA
IgG
IP
PriA
IgG
1 2 3 4 5 6 7 8 9 10 11 12
D
PriA (1 ng)
IP
PriA
IgG
PriA
IgG
thymine
2 3 4 5
E
AQ634 priA+ thyA
inverted
normal growth
thymine starvation
log2 (IP/input)
+4
+2
+1
0
-1
0
1.0
2.0
3.0
4.0
MB
TerE
TerA
TerD
TerC
TerB
TerF
oriC
F
AQ8851 priA1::kan thyA
normal growth
thymine starvation
log2 (IP/input)
oriC

Figure 1

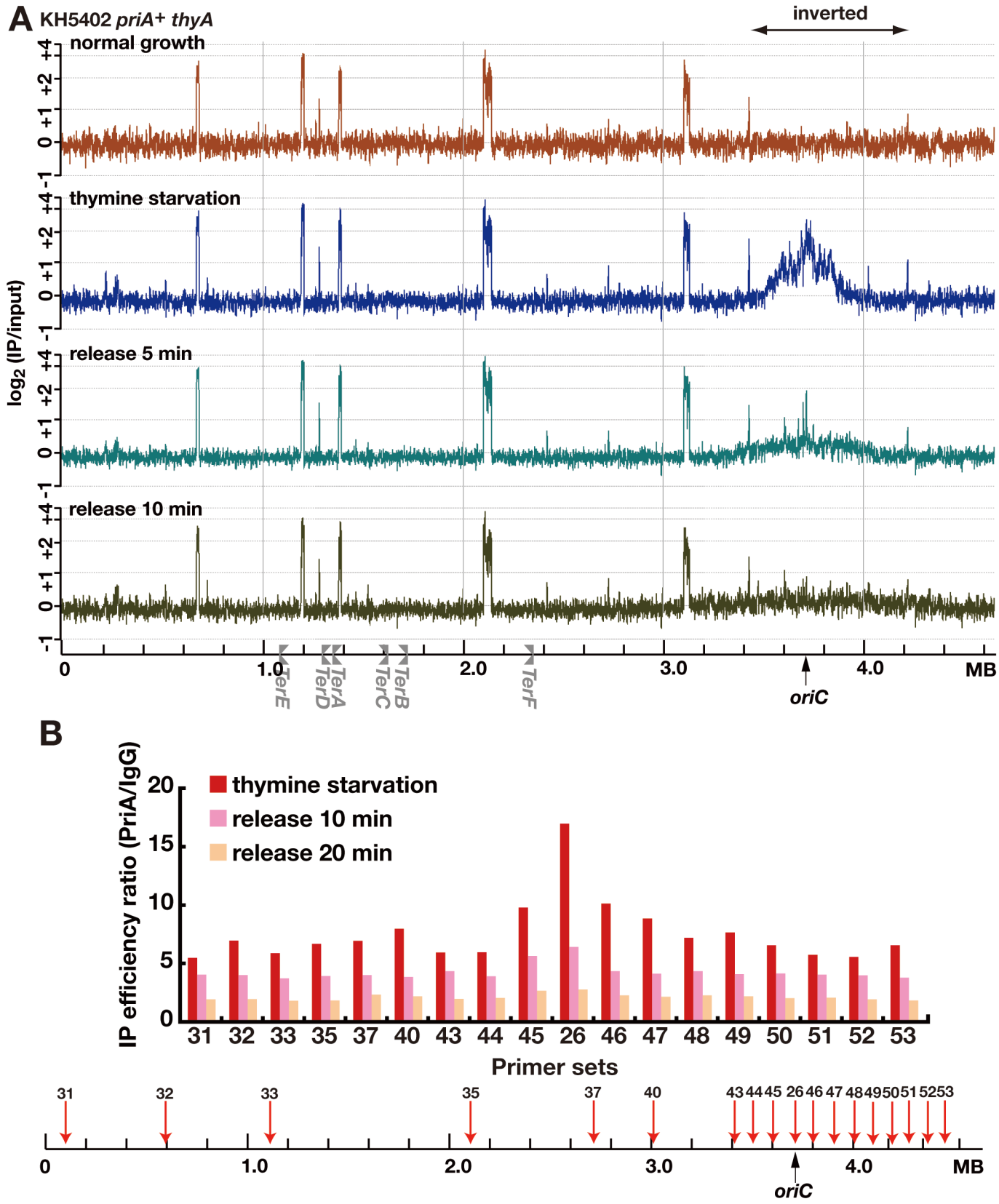
A
KH5402 priA+ thyA
inverted
normal growth
thymine starvation
release 5 min
release 10 min
log2 (IP/input)
+4
+2
+1
0
-1
TerE
TerA
TerD
TerC
TerB
TerF
oriC
0
1.0
2.0
3.0
4.0
MB
B
IP efficiency ratio (PriA/IgG)
thymine starvation
release 10 min
release 20 min
20
15
10
5
0
31 32 33 35 37 40 43 44 45 26 46 47 48 49 50 51 52 53
Primer sets
31 32 33 35 37 40 43 44 45 26 46 47 48 49 50 51 52 53
oriC
MB

Figure 2

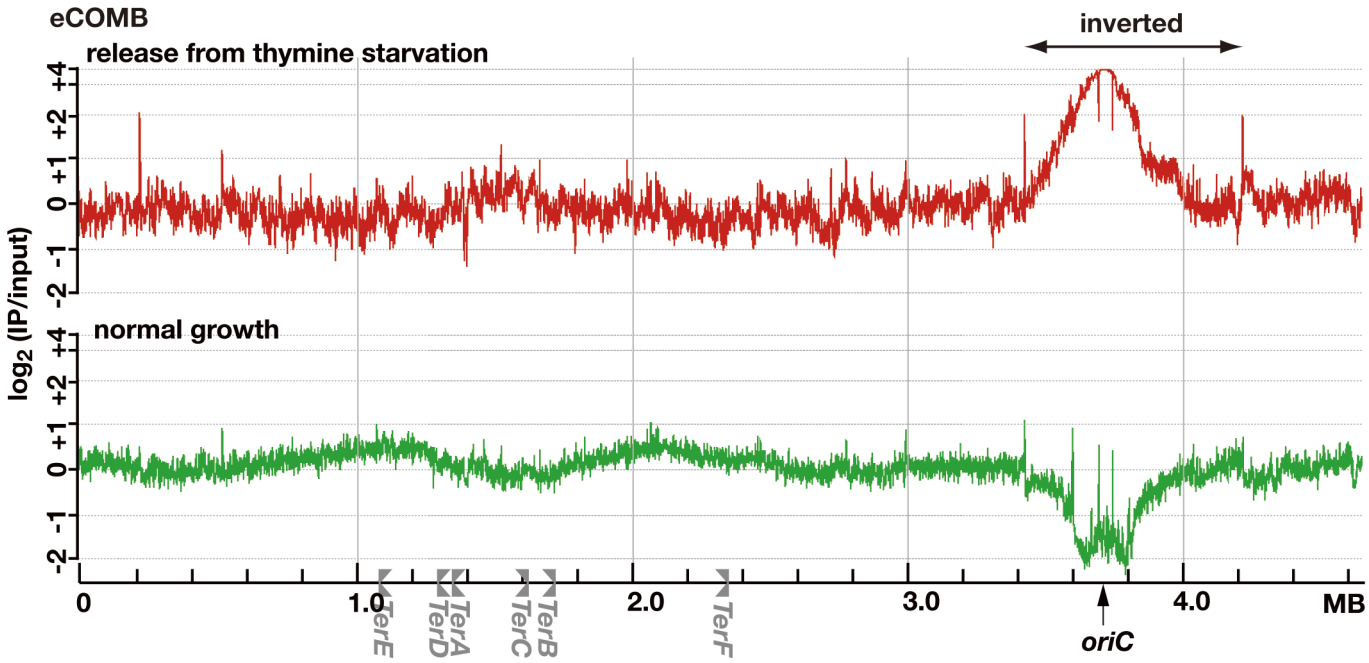
eCOMB
release from thymine starvation
inverted
log2 (IP/input)
+4
+2
+1
0
-1
-2
normal growth
0
1.0
2.0
3.0
4.0
MB
TerE
TerA
TerD
TerB
TerC
TerF
oriC

Figure 3

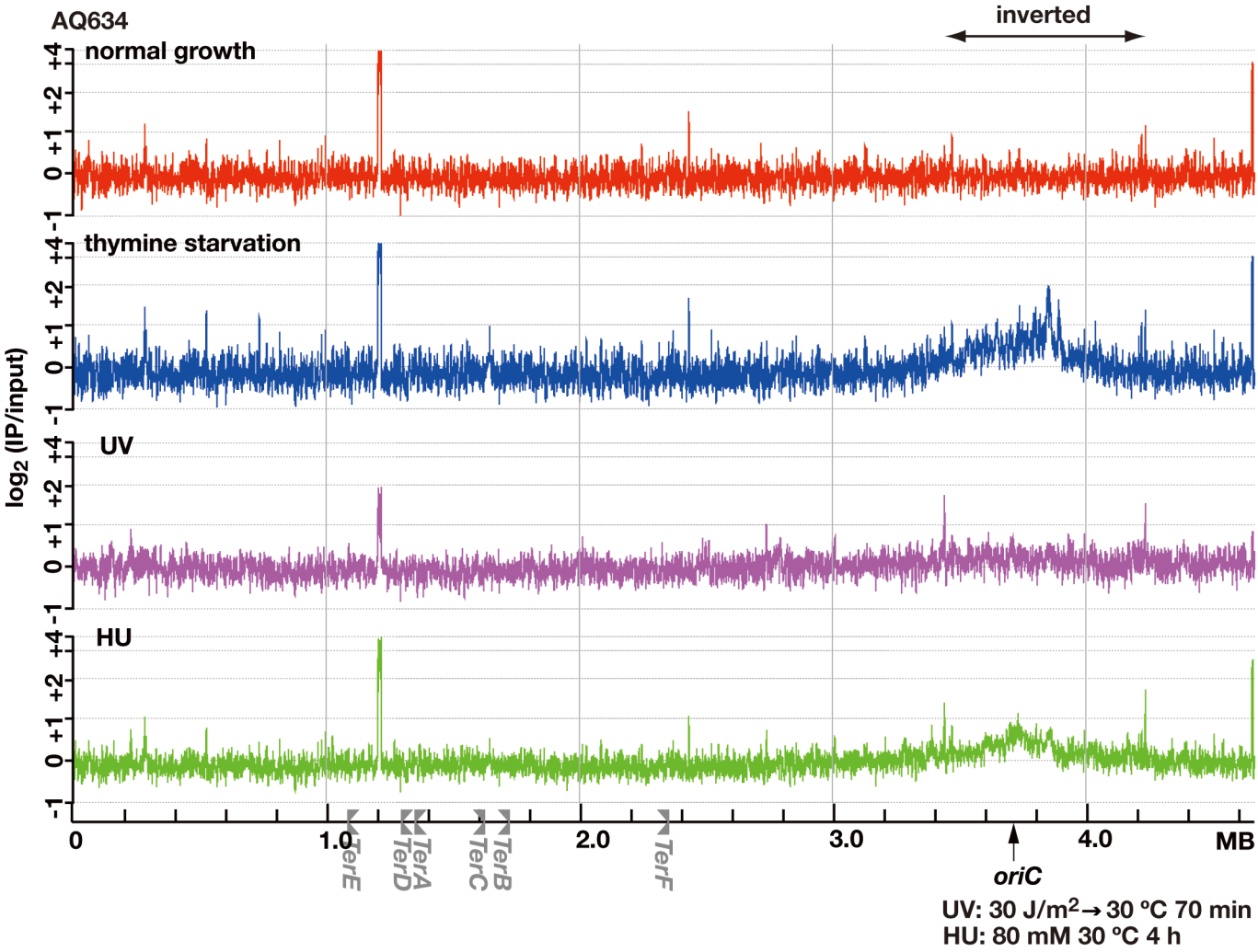
AQ634
inverted
normal growth
thymine starvation
UV
HU
log2 (IP/input)
+4
+2
+1
0
-1
0
1.0
2.0
3.0
4.0
MB
TerE
TerA
TerD
TerB
TerC
TerF
oriC
UV: 30 J/m2→ 30 °C 70 min
HU: 80 mM 30 °C 4 h

Figure 4

Supplementary Material

Materials and Methods

Strains and oligonucleotides

Bacterial strains and oligonucleotides used in this study are summarized in **Supplementary Table 1**.

Media

Strains were grown in LB or M9 media (M9 supplemented with required amino acids, 20 μg/ml thymine, and 0.4% glucose) or M9CAA (M9 supplemented with 0.2% casamino acid, 50 μg/ml tryptophan, 20 μg/ml thymine, and 0.4% glucose).

Anti-PriA antibody

The PriA full-length protein was overexpressed, purified as described previously [30] except that the final heparin fraction was further purified by MonoQ column (GE healthcare) and flow though fractions were collected as the final purified material, and were used as antigen for development of rabbit polyclonal antibody. Antisera obtained from immunized rabbits were purified with the same antigen by using NHS-activated HP column (GE healthcare) according to the manufacturer.

Immunoprecipitation with anti-PriA antibody

Lysates were incubated with 0.5 μg of PriA antibody or normal rabbit IgG (Santa Curz Biotechnology) and proteins bound to nProteinA Sepharose FF beads (GE healthcare) were extracted by washing with SDS-PAGE sample buffer. A half of the eluate was loaded onto 12% SDS-PAGE. Gel was visualized by silver staining or PriA was detected by Western blotting with anti-PriA antibody serum or purified anti-PriA antibody.

Thymine starvation

Strains carrying *thyA* mutation was incubated in LB or M9 media and exponential growing cells were harvested, washed with M9 salt (M9 without any nutrients) and released into the same medium without thymine. After incubation for 3 h,

immunoprecipitation was conducted as described above.

Microarray analyses

Microarray slide was designed and produced by Agilent Technology Limited (custom number #035583). Probes were arrayed in 4 x 44 k format. Each probe size is 60 nucleotides and distances between probes are ~ 100 bp.

ChIP-on-chip analyses

Cells growing exponentially in M9 media at 30 ºC were thymine starved for 3 hrs. In release from thymine starvation, DNA synthesis was restarted by addition of 8 µg/ml thymine along with 200 µg/ml rifampicin and 150 µg/ml chloramphenicol. Cells were harvested at the times indicated after release, and immunoprecipitation was conducted as follows. To the 200 ml culture, 50 ml of the 5x fix solution (5% formaldehyde in 50 mM sodium phosphate buffer) was added and incubated for 10 min at room temperature, washed twice with PBS and treated in 0.5 ml (per OD_{600} = 0.1) of 2 mg/ml of lysozyme in solution A (10 mM Tris-HCl [pH 8.0], 10 mM EDTA, 500 mM NaCl, 10% sucrose, and 2 mM DTT) for 1 hr on ice. After addition of an equal volume of 2 x IP buffer (100 mM Tris-HCl [pH 7.0], 10 mM EDTA, 500 mM NaCl, 2% Triton X-100, 1 mM PMSF), cells were divided into 1.5 ml tubes (1 ml of the sample each) and subjected to three times repeat of freeze/thaw cycle and sonication (amplitude 35%, 6 repeats [with 3 min intervals] of 15 cycle of "0.4 sec on and 0.6 sec off"). After centrifugation, antibodies (2 µg) were added to 250 µl of lysate diluted to 1 ml with 1 x IP buffer. A part of lysate (40 µl) was collected for "input DNA" sample. After incubation for 1 hr at room temperature, 35 µl of nProtein A Sepharose FF beads (GE healthcare) as 50% slurry (17.5 µl as beads) was added. After incubation for 1 hr at room temperature, beads were recovered and washed with 1 ml of ice-cold 1 x IP buffer four times and 1 ml of TE twice and dissolved in 50 µl of 1% SDS/TE. After incubation at 65 ºC for 30 min, supernatant was recovered in a new tube. The collected "Protein-DNA complexes (immunoprecipitate; IP)" and "input DNA" fractions were further incubated at 68 ºC for 12 hrs after addition of 150 µl of TE with 1% SDS to reverse cross-linking. The samples were further incubated in 400 µl of 0.5% SDS, 200 mM NaCl, 50 µg/ml glycogen, and 200 µg/ml RNaseA (final concentration) at 37 ºC for 1 hr to remove RNAs. After addition of 0.5 mg/ml Proteinase K and incubation at 65°C for 2 hrs, the

samples were extracted by phenol, precipitated with ethanol and purified by using MinElute Reaction Cleanup Kit (QIAGEN). Purified DNA was eluted by 20 µl or 40 µl of TE for the immunoprecipitate or input DNA sample, respectively, and used for amplification with GenomePlex Complete WGA Kit (Sigma-Aldrich) according to instruction from manufacturer. Amplified DNA samples were labeled and scanned by Agilent SureScan Microarray Scanner (Agilent) and signals were quantified by Agilent Feature Extraction software. Intensity of the IP sample was divided with that of input DNA and values were plotted as log ratio by Genomic Workbench software (Agilent). We have used the genome sequence of K-12 W3110 (accession number, AC_000091.1) as a reference sequence. This strain has an inversion between *rmD* and *rrnE* [31,32] and *oriC* is located on the complement strand (3710706-3710937).

Quantitative PCR

Lysate preparation and immnoprecipitation were performed as described above. KH5402-1 (*thyA*) was grown in M9CAA without thymine for 3 hrs and DNA synthesis was released by addition of 8 µg/ml thymine along with 200 µg/ml of rifampicin and 150 µg/ml of chloramphenicol. Real-time PCR was conducted with SYBR Premix Ex Taq (TaKaRa Bio) on a LightCycler 480 (Roche) using primer sets shown in **Supplementary Table 1**.

BrdU incorporation

eCOMB (Δ*thyA* Δ*yjjG-deoB*), kindly provided by Dr. Akiyama at Nara Institute of Science and Technology, was grown in M9CAA supplemented with 2 µg/ml thymidine and washed with M9 salt for thymine starvation. After 3 hr starvation of thymine, cells were released into M9CAA with 50 µg/ml BrdU, and 150 µg/ml chloramphenicol for 2 min. DNA synthesis was terminated by addition of 2% sodium azide and cells (200 ml) were collected for DNA preparation. For labeling in normal cells, 50 µg/ml BrdU was added to eCOMB cells exponentially growing in M9CAA for 5 min before harvest of the cells (50 ml). Chromosomal DNA was sheared with sonication and fragmented DNA was used for immunoprecipitation with 2 µg anti-BrdU antibody (MBL). Precipitated DNA was analyzed on microarray after amplification as above.

Indirect immunofluorescence microscopy

Immunostaining was conducted as described previously [33]. In brief, exponential growing AQ634 (*priA*$^+$ *thyA*) or AQ8851 (*priA1::kan thyA*) cells were fixed with 80% ice-cold methanol overnight, collected and spotted onto APS coated slide glass. Immobilized cells were treated with 2 mg/ml lysozyme in 25 mM Tris-HCl (pH 8.0), 50 mM glucose, and 10 mM EDTA for 5 min at room temperature. After wash with -20 ºC methanol and acetone, slide was dried and blocked with 2% BSA in PBSTE (PBS containing 0.01% Tween 20 and 10 mM EDTA) for 20 min at room temperature. The blocking regent was removed and treated with 30 μl of 6 μg/ml affinity purified anti-PriA antibody for 1 hr at room temperature with cover glass in moisture chamber. After washing with 2.5 ml of PBSTE, the second-step antibody, anti-rabbit IgG (goat) labeled with Alexa 546 (Life Technologies), diluted to 500 fold with 2% BSA in PBSTE and precleared with the lysate from KH5402-1 to remove any antibodies cross-reacting with *E. coli* cells, was overlaid onto cells and incubation was continued with cover glass for 1 hr in a dark box. The cells were washed with 2.5 ml of PBSTE and also stained with 10 μg/ml of DAPI for 1 min and, after wash with PBSTE, mounted with mounting medium (Fluoromount/Plus, Diagnostic BioSystems). Slide glasses were stored at -30 ºC in dark box until observation. Pictures were taken with an appropriate filter set for Alexa (PriA) or DAPI (nucleoid). Phase contrast was also monitored to detect cell shapes.

UV irradiation

Exponentially growing cells (AQ634; 200 ml) were harvested and resuspended in 15 ml of M9 salt. Cell suspension were placed in a clear 10 cm dish, irradiated by UV (254 nm) at 30 J/m^2, and returned to 200 ml of M9CAA for further incubation for 70 min. The cells were placed in dark in the 70 min post-incubation period to prevent photoreactivating reactions.

Legends to Supplementary Figures

Supplementary Figure S1. Western blotting analysis with serum or purified antibody against *Escherichia coli* PriA protein. To determine antibody specificity, anti-serum (serum [1/1000 dilution], lanes 1 - 8) or affinity purified antibody (purified Ab [100 ng/ml], lanes 9 - 16) was used in Western blotting on the indicated samples which were run on 12% SDS-PAGE. Lysates, IP (immunoprecipitates) and IP sup (supernatants after immunoprecipitation), derived from 5 x 10^7, 1 x 10^9 and 5 x 10^7 cells, respectively, were loaded onto gel. Purified PriA protein (10 ng) was also applied as a control (indicated by arrow) in each set (lanes 1 and 9). The positions of molecular weight marker are indicated to the left of the gel.

Supplementary Figure S2. Indirect immunofluorescence microscopy of PriA protein. Immunostaining of PriA protein was conducted as described in the text. Exponentially growing AQ634 (*priA*$^+$ *thyA*) and AQ8851 (*priA1::kan thyA*) as well as BL21 harboring pRA45 (expressing the full-length priA gene under control of T7 promoter [34]; transcription induced by addition of IPTG for 3 hrs) cells were fixed with methanol, incubated with anti-PriA antibody and then with Alexa 546 to visualize PriA protein (red; see "Materials and methods"). Cells were also stained with DAPI to visualize nucleoid (blue). The right-most panel shows cell shape (phase contrast). A portion of the image (shown by small squares) is enlarged in the left-upper insets.

Supplementary Table 1 *E. coli* strains and primers used in this study

Strain	Relevant genotype	Source of reference
AQ634	*thyA*	[35]
AQ8851	*thyA priA1::kan*	[35]
KH5402-1	*ilv thyA thr thrA[amber] trpE9829[amber] metE deo supF[Ts]*	[36]
eCOMB	*ΔthyA ΔyjjG-deoB*	[20]

Primer	Sequence (5' -3')
26 fwd	ATCAGGCGGGTATCCAGTTTAGGAT
26 rev	CTTCAGTCCCATTTGGGTAACAGCA
31 fwd	GCGAACGCTGTTTTCTTAAGCACT
31 rev	AGTTAACTTTGGCTGAAGGCTCGTG
32 fwd	GATAATAAAACGCGCTGGCAGGTGA
32 rev	CAGCAACAGCGGATGATAAACACGA
33 fwd	ATGATGTCGCAAAGCAAGCTCAATC
33 rev	CCGAAAGTGAAATAATCCGGGCTGT
35 fwd	ATGTTAGTCGCTGCCAAAGAGATCG
35 rev	AAGCCGCAAGTGGTGGGTATTTATC
37 fwd	TTCAGTACCGGCACAACTTCGAGAT
37 rev	ATTACCATCAAAGCGCAAAGCGTG
40 fwd	TTCCGCTCAACTTATGGATTGCACG
40 rev	ATTGCATAACATTCAGGGCCGACA
43 fwd	TTTTTGCCGGAGGATAGCAGCAGAT
43 rev	AATGCGTACTGACTCTTCGCCTTCA
44 fwd	AACAAACAACACGCGATAGCAACC
44 rev	ACCGATCCATCTTTCCAGCACCTAT
45 fwd	ATTCGCGGGCGCATTTTGTTATCT
45 rev	TGAATCTTTCTCTGGCCTGACCACT
46 fwd	TGTGAATATTTTGGTGGCACGGGA
46 rev	TACTCTCTTTGCTGTTGCTGGGGAT
47 fwd	ATTGGGCGGTGAAAACTATGTCCTG
47 rev	ACTGTTTCAGGAAGCCATAGACCGT
48 fwd	ATCGCAATCATCATGCGCTGCAACA
48 rev	AAATTGCCACCATCATGCAGAACCC
49 fwd	ACTTCTACGCCAGCACCAAAAGAGA
49 rev	GCTGACCATTACGCGTCGTTTCATA
50 fwd	GTACGAATAGTTGGGCAAGCAAGGT
50 rev	AACGCAGACCTGGGATGATTACACA
51 fwd	ACTAAATACTGGCGCAGCCTGTTGA
51 rev	ACACAAACAGGGCAACACTACCAAG
52 fwd	AAAAAGATGGCTTACGCTTTCGGC
52 rev	TCACGAAGGCAAGGTTTACGAACTG
53 fwd	AGGACTTAATGCCGATACACCCCAT
53 rev	AATTCAGGCGTCAGGCAAAAGAGGT

Primer sets (frd and rev) used for ChIP-qPCR in Figure 3B at each genomic location are listed.

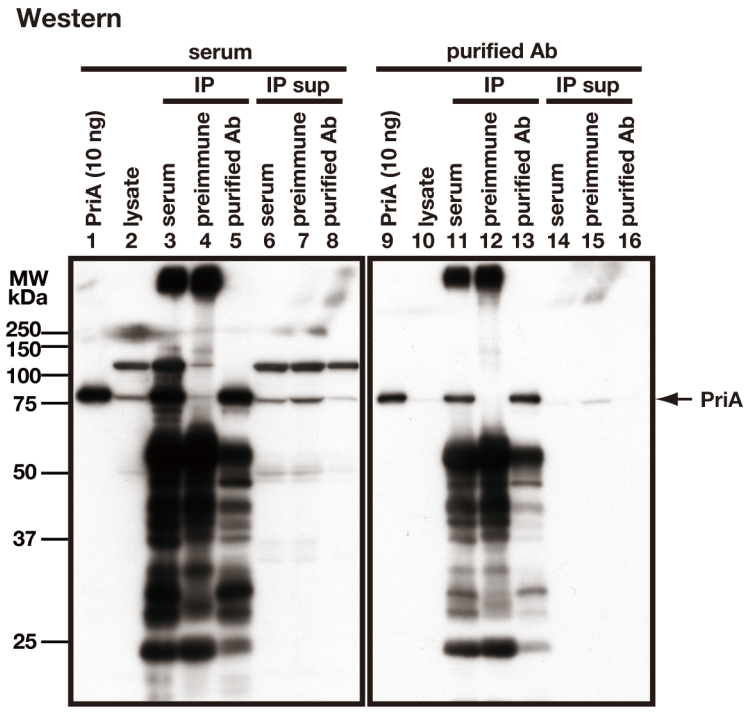

serum; anti-PriA serum, 8 weeks after immunization
preimmune; serum before immunization, 0 week
purified Ab; affinity purified PriA antibody
IP sup; supernatant after IP

Supplemetary Figure S1

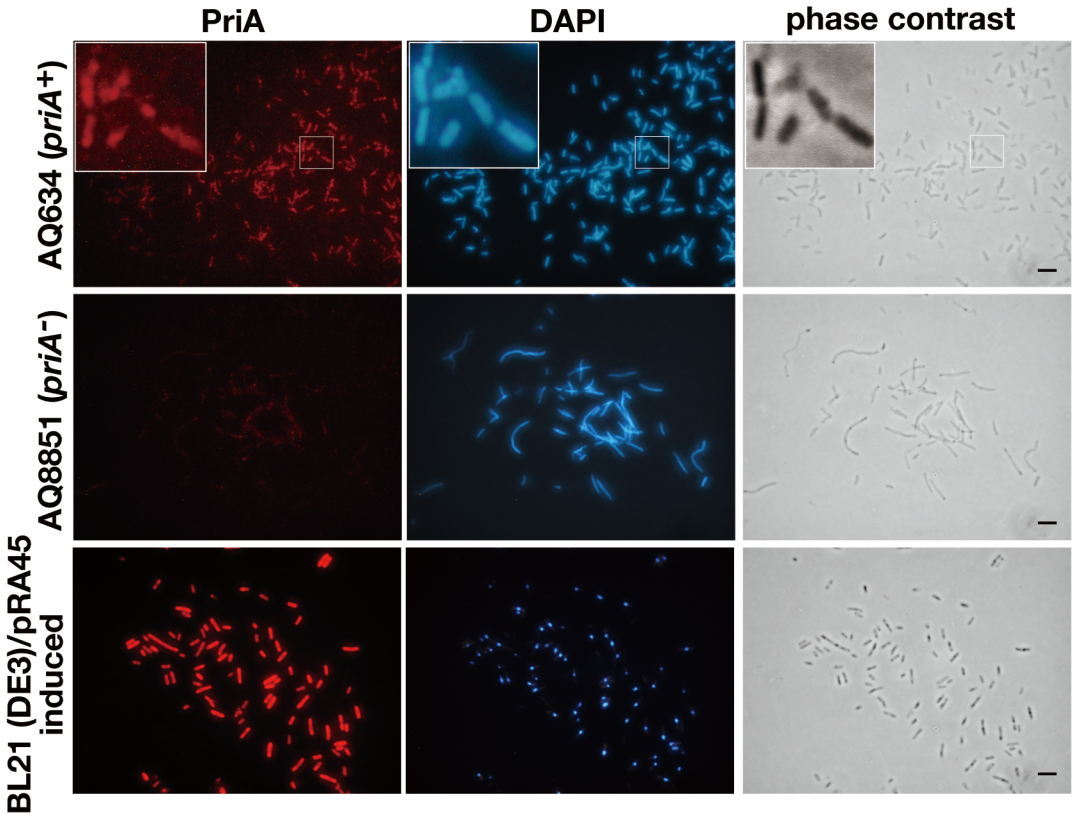

Supplemetary Figure S2